J Supercond Nov Magn (2015) 28:2009–2015
DOI 10.1007/s10948-015-2998-5

ORIGINAL PAPER

Significance of Phonon Modes and Excess Conductivity of $(Cu_{0.5}Tl_{0.5})Ba_2Ca_3(Cu_{4-x}Ti_x)O_{12-\delta}$ ($x = 0, 0.25, 0.50, 0.75, 1.0$) Superconductors

Nawazish A. Khan · S. Qamar Abbas · M. Nasir Khan

Received: 6 January 2015 / Accepted: 23 January 2015 / Published online: 1 March 2015

Abstract We have synthesized $(Cu_{0.5}Tl_{0.5})Ba_2Ca_3(Cu_{4-x}Ti_x)O_{12-\delta}$ ($x = 0, 0.25, 0.50, 0.75, 1.0$) superconductors by two-step solid-state reaction method at 880 °C. The a-axis length of tetragonal unit cell increases, whereas the c-axis decreases with doping of Ti in the final compound revealed by X-ray diffraction measurements. Moreover, the magnitude of superconductivity suppresses with increased Ti doping. The Fourier transform infrared spectrometer (FTIR) absorption measurements have shown that the peak position of the apical oxygen modes at 480 and 540 cm^{-1} remains unchanged, whereas the CuO_2/TiO_2 planar oxygen modes is softened with increased Ti doping. We explained the softening of planar oxygen mode to be arising due to the difference in the atomic masses of Ti (47.90 amu) and Cu (63.54 amu) atoms. The suppression of superconductivity magnitude is suggested to be originating from an-harmonic oscillations induced by doped Ti atoms which in turn suppress the density of phonon population. These studies show the importance of density of phonon population in mechanism of high-T_c superconductivity and hence the electron-phonon interactions. The excess conductivity analyses (FIC) of conductivity data of these samples have shown that with increased Ti doping, the mean field critical temperature T_{cmf} is shifted to lower temperatures. The increase in the coherence length along the c-axis, interlayer coupling, and the Fermi velocity is suggested to be arising from the decrease in the c-axes length. We attribute the suppression in B_c, B_{c1}, $J_{c(0)}$, and τ_ϕ with Ti doping to the free energy difference between the normal and superconducting state. The idea of suppression in the density of phonon modes induced by Ti doping is supported by excess conductivity analyses.

Keywords Ti-doped superconductors · Phonon modes · Electron-phonon interactions

N. A. Khan (✉) · S. Qamar Abbas
Materials Science Laboratory, Department of Physics,
Quaid-i-Azam University, Islamabad 45320, Pakistan
e-mail: nawazishalik2@yahoo.com

M. Nasir Khan
Physics Division, PINSTECH, P.O. Nilore,
Islamabad 45600, Pakistan
e-mail: nakhan@qau.edu.pk

1 Introduction

The superconductivity in oxides is confined in CuO_2 planes, whereas the carriers are supplied by $Cu_{0.5}Tl_{0.5}Ba_2O_{4-\delta}$ charge reservoir layers [[1, 2], and references therein]. Copper atoms in the CuO_2 planes where superconductivity lies are in the $3d^9$ state, which provide the skeleton of covalent bonding, and the metallic character arises from the delocalized $4s^2$ electrons [3, 4]. Since the wave function spread of $4s^2$ electrons is extended to many interatomic spacing, these compound show enough density of carriers at room temperature and hence the metallic behavior from room temperature down to onset of superconductivity. The possibility of existence of electron-phonon interaction in oxide superconductors is quite possible; however, the oxygen isotope effect measurements have ruled out any role of oxygen atoms of such mechanism. This shows that any role of the hard phonons in mechanism of high-T_c superconductivity is minimal. In order to look into the possibility of soft phonons in the mechanism of high-T_c superconductivity [5], we have doped the Ti at Cu sites in CuO_2 planes of $(Cu_{0.5}Tl_{0.5})Ba_2Ca_3(Cu_{4-x}Ti_x)O_{12-\delta}$ ($x = 0, 0.25, 0.50, 0.75, 1.0$) superconductors. The substitution of this atom at the copper site will be helpful in understanding the role of

phonon interaction in the mechanism of high-temperature superconductivity [6–8]. Titanium atom has ground state electronic configuration $3d^2 \cdot 4s^2$ and atomic mass of the Ti (47.9 amu) which is smaller than the Cu (63.5 4amu) atoms. Due to this difference in masses, it is likely that doped Ti atoms may induce an-harmonic oscillations which will suppress the density of phonon in CuO_2/TiO_2 planes. These experiments will be helpful in determining the pivotal role of electron-phonon interactions in the mechanism of high-T_c superconductivity.

2 Experimental

$(Cu_{0.5}Tl_{0.5})Ba_2Ca_3(Cu_{4-x}Ti_x)O_{12-\delta}$ ($x = 0$, 0.25, 0.50, 0.75, 1.0) samples were synthesized by two-step solid-state reaction method. In the first stage, $Cu_{0.5}Ba_2Ca_3(Cu_{4-x}Ti_x)O_{12-\delta}$ ($x = 0$, 0.25, 0.50, 0.75, 1.0) precursor material was synthesized mixing weighted amounts of TiO_2, $Ba(NO_3)_2$, $Ca(NO_3)_2 \cdot 4H_2O$, and Cu(CN) in a quartz mortar pestle followed by firing at 880 °C in a quartz boat for 24 h. These samples were furnace cooled to room temperature and ground again for an hour and again fired at 880 °C in an alumina boat for 24 h. These samples were furnace cooled to room temperature after each heat treatment. The precursor material was again ground for about an hour and mixed with Tl_2O_3 to give $(Cu_{0.5}Tl_{0.5})Ba_2Ca_3(Cu_{4-x}Ti_x)O_{12-\delta}$ ($x = 0$, 0.25, 0.50, 0.75, 1.0) as final reactants composition and pelletized under 3.8 tons/cm^2. The pellets were then wrapped in a gold capsule and annealed for about 18 min at 880 °C and then quenched to room temperature after the heat treatment. The superconductivity characteristics of the samples were measured by resistivity, AC susceptibility, and Fourier transform infrared spectroscopic measurements. The Fourier transform infrared spectroscopic (FTIR) measurements absorption measurements were carried out by using Nicolet 5700 Fourier Transform Infrared Spectrometer (FTIR) in 400–700 cm^{-1} wave number range.

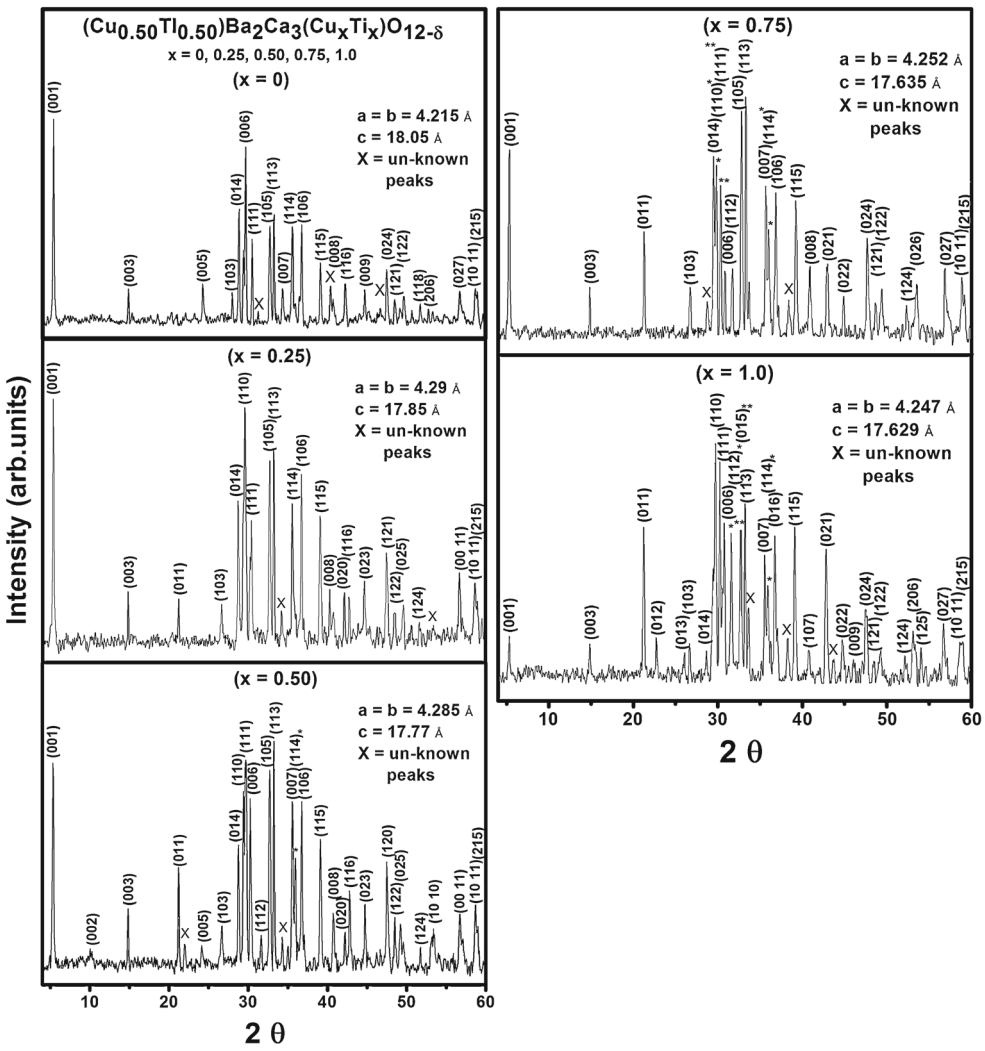

Fig. 1 **a**, **b**, **c** X-ray diffraction pattern of $(Cu_{0.5}Tl_{0.5})Ba_2Ca_3(Cu_{4-x}Ti_x)O_{12-\delta}$ ($x = 0$, 0.25, 0.50) samples. **d**, **e** X-ray diffraction pattern of (Cu0.5Tl0.5)Ba2Ca3(Cu4 $-x$ Ti x) O12 $-\delta$ ($x = 0.75$,1.0) samples

The crystal structure of the samples was measured by X-ray diffraction scan using Bruker DX 8 Focus employing CuKα radiations of wavelength 1.54056 Å. The cell parameters were determined by check cell computer refinement program.

3 Results and Discussion

3.1 (a) Ti-Doped $(Cu_{0.5}Tl_{0.5})Ba_2Ca_3(Cu_{4-x}Ti_x)O_{12-\delta}$ ($x = 0, 0.25, 0.50, 0.75, 1.0$) Samples

The X-ray diffraction scans of $(Cu_{0.5}Tl_{0.5})Ba_2Ca_3(Cu_{4-x}Ti_x)O_{12-\delta}$ ($x = 0, 0.25, 0.50, 0.75, 1.0$) samples are shown in Fig. 1a–e. The planar reflections are best fitted to the tetragonal crystal structure following P4/MMM space group. The c-axis length suppresses, whereas the a-axis length increases with Ti doping (Fig. 2). The resistivity versus temperature measurements of as-prepared $(Cu_{0.5}Tl_{0.5})Ba_2Ca_3(Cu_{4-x}Ti_x)O_{12-\delta}$ ($x = 0, 0.25, 0.50, 0.75, 1.0$) samples are displayed in Fig. 3. These samples have shown room temperature resistivity around 0.041, 0.231, 0.111, 0.186, and 0.110 Ω cm, respectively. The smaller room temperature resistivity values are an indication of lower density of defects in the final compounds.

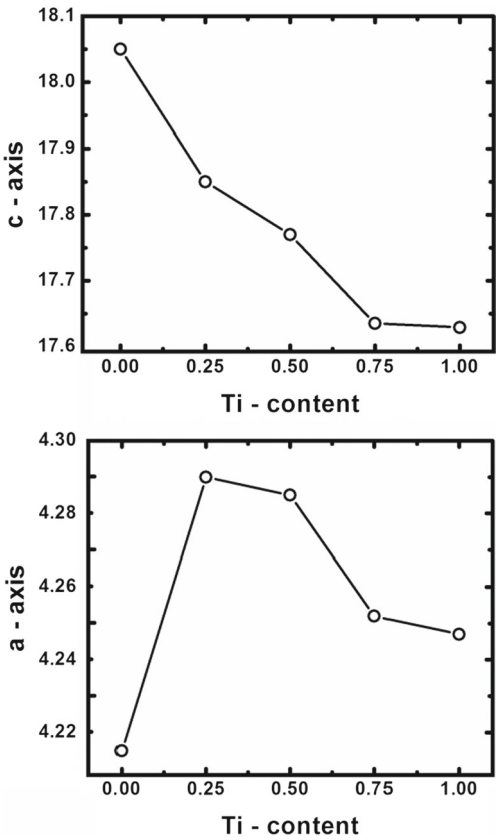

Fig. 2 Variation in the c-axis and a-axis because of Ti content

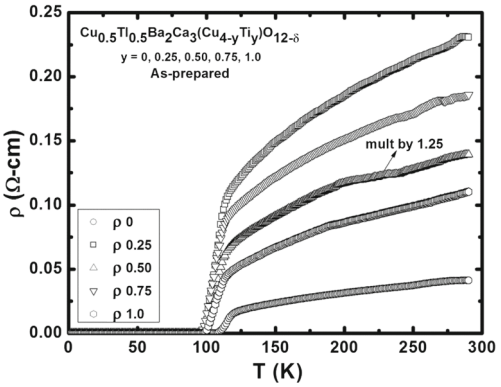

Fig. 3 Combined resistivity of as-prepared $(Cu_{0.5}Tl_{0.5})Ba_2Ca_3(Cu_{4-x}Ti_x)O_{12-\delta}$ ($x = 0, 0.25, 0.50, 0.75, 1.0$) samples

The metallic variation of resistivity from room temperature down to onset temperature of superconductivity is typical feature of these samples. These samples have shown onset of superconductivity around 124.6, 118.7, 117.7, 116.1, and 120 K and $T_c(R = 0)$ at 108.4, 100.1, 97, 94.4, and 99 K, respectively. AC magnetic susceptibility measurements of $(Cu_{0.5}Tl_{0.5})Ba_2Ca_3(Cu_{4-x}Ti_x)O_{12-\delta}$ ($x = 0, 0.25, 0.50, 0.75, 1.0$) samples are displayed in Fig. 4. It can be seen from this figure that the magnitude of the superconductivity is suppressed with Ti doping in the final compound. The onset of superconductivity is observed around 105.6, 114.3, 103.7, 115.2, and 102.4 K, respectively.

The FTIR absorption measurements of $(Cu_{0.5}Tl_{0.5})Ba_2Ca_3(Cu_{4-x}Ti_x)O_{12-\delta}$ ($x = 0, 0.25, 0.50, 0.75, 1.0$) samples are displayed in Fig. 5. Three absorption bands around 484, 538–539, and 598–582 cm^{-1} can be seen in these spectra. The former two modes are related to the vibrations related to apical oxygen atoms, whereas the third one is associated with the vibrations of planar oxygen atoms [9, 10]. The peak position of the apical oxygen modes is not appreciably changed, but the planar oxygen mode

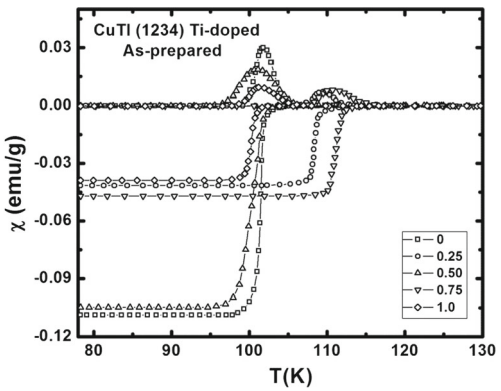

Fig. 4 The AC susceptibility versus temperature measurements of as-prepared $(Cu_{0.5}Tl_{0.5})Ba_2Ca_3(Cu_{4-x}Ti_x)O_{12-\delta}$ ($x = 0, 0.25, 0.50, 0.75, 1.0$) samples

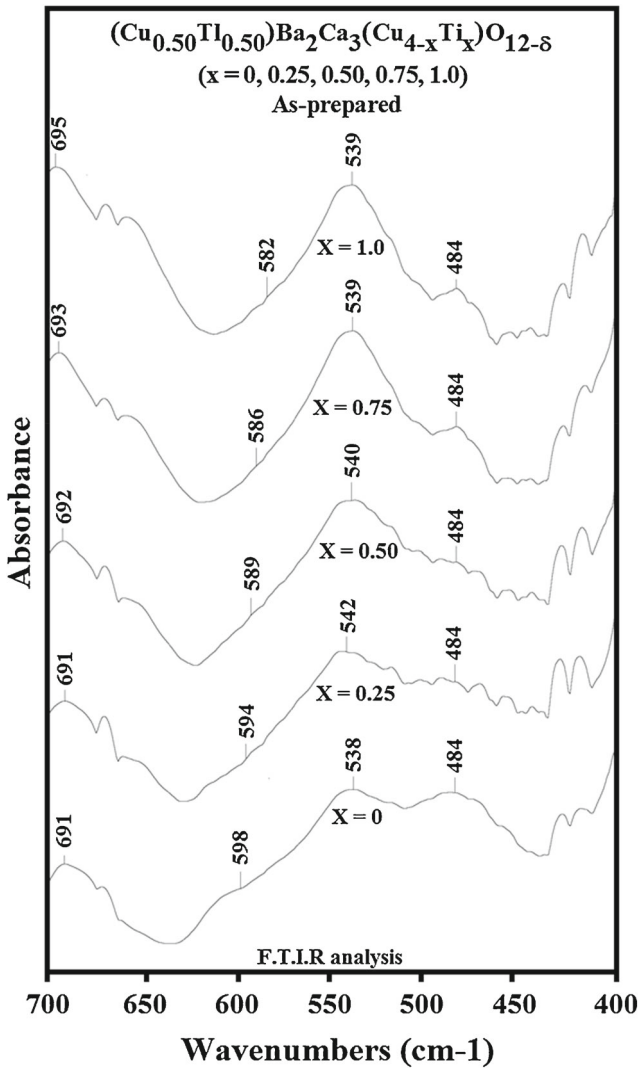

Fig. 5 FTIR measurements of as-prepared $(Cu_{0.5}Tl_{0.5})Ba_2Ca_3(Cu_{4-x}Ti_x)O_{12-\delta}$ ($x = 0, 0.25, 0.50, 0.75, 1.0$) samples

is systematically softened with increased Ti doping. Planar oxygen mode in $(Cu_{0.5}Tl_{0.5})Ba_2Ca_3(Cu_{4-x}Ti_x)O_{12-\delta}$ ($x = 0, 0.25, 0.50, 0.75, 1.0$) samples is observed around 598, 594, 589, 586, and 582 cm^{-1}, respectively. The most likely reason for the softening of planar oxygen mode is the smaller mass of the doped Ti atoms. The atomic mass of Ti (47.90 amu) is smaller than Cu (63.54 amu) atoms that promotes an increase in the bond length of planar oxygen atoms and make them oscillate at the lower wavenumbers.

3.2 (b) Excess Conductivity Analyses $(Cu_{0.5}Tl_{0.5})Ba_2Ca_3(Cu_{4-x}Ti_x)O_{12-\delta}$ ($x = 0, 0.25, 0.50, 0.75, 1.0$) Samples

The temperature dependence of conductivity around T_c and beyond it follows the relationship of the form $\Delta\sigma_{(T)} = \Delta\sigma_{RT}\varepsilon^{-\lambda D}$. The analyses of excess conductivity $\Delta\sigma_{(T)}$ are done by converting this relationship into equation which identical to the Arrhenius relation:

$$\ln\Delta\sigma_{(T)} = \ln\Delta\sigma_{RT} - \lambda_D \ln(\varepsilon) \quad (1)$$

Here, the $\varepsilon = \left[\frac{T - T_c^{mf}}{T_c^{mf}}\right]$ is the reduced temperature and the λ_D is dimensional exponent.

The mean field critical temperature T_c^{mf} is determined from the point of inflection of the temperature derivative of resistivity ($d\rho/dT$). Depending upon the values of λ_D, the dimensional exponent explains various thermally activated processes in three, two, and one dimensions. The λ_D value around 0.33 corresponds to critical regime, 0.5 three-dimensional conductivity (3D), 1.0 two-dimensional (2D), and 2.0 for zero-dimensional (0D) conductivity, respectively [11–14]. At the junction of various thermally activated processes, three crossover temperatures are found, i.e., T_G, T_{3D-2D}, and T_{2D-0D}. The T_G is the crossover temperature of Ginzburg-Landau regime with three-dimensional conductivity regimes, the T_{3D-2D} is the crossover temperature of three-dimensional conductivity regime with two-dimensional conductivity regimes, and the T_{2D-0D} is the crossover temperature of two-dimensional conductivity regime with zero-dimensional conductivity regimes. Various crossover temperatures derived from the log plot of the excess conductivity versus the reduced temperature are mentioned in the Fig. 6 a–e and Table 1. The values of various exponents such as, λ_{cr}, λ_{3D}, λ_{2D}, and λ_{0D} are given in Table 2.

The Aslamazov-Larkin theory [14] is used for the excess conductivity analysis of thin film samples, whereas for the polycrystalline samples the Lawrence and Doniach (LD) model is employed [15]. The following is the expression of the Lawrence and Doniach (LD) model:

$$\Delta\sigma_{LD} = [e^2/(16\hbar d)](1 + J\varepsilon^{-1})^{-1/2}\varepsilon^{-1} \quad (2)$$

In this expression, the $J = [2\xi_{c(0)}/d]^2$ is interlayer coupling, d is the thickness of superconducting layers ($\sim$ 18 Å in present case), and the $\xi_{c(0)}$ is coherence length along the c-axis. The excess conductivity analyses of conductivity data of $(Cu_{0.5}Tl_{0.5})Ba_2Ca_3(Cu_{4-x}Ti_x)O_{12-\delta}$ ($x = 0, 0.25, 0.50, 0.75, 1.0$) samples have shown that the coherence length along the c-axis, the Fermi velocity of the carriers and the interlayer coupling J increase with the doping of Ti in the final compounds. The enhancement in the value of these parameters is most likely associated with the decrease in the c-axis length with doping of Ti (see Table 2).

The Ginzburg number N_G is determined from the crossover temperature T_G of critical and three-dimensional

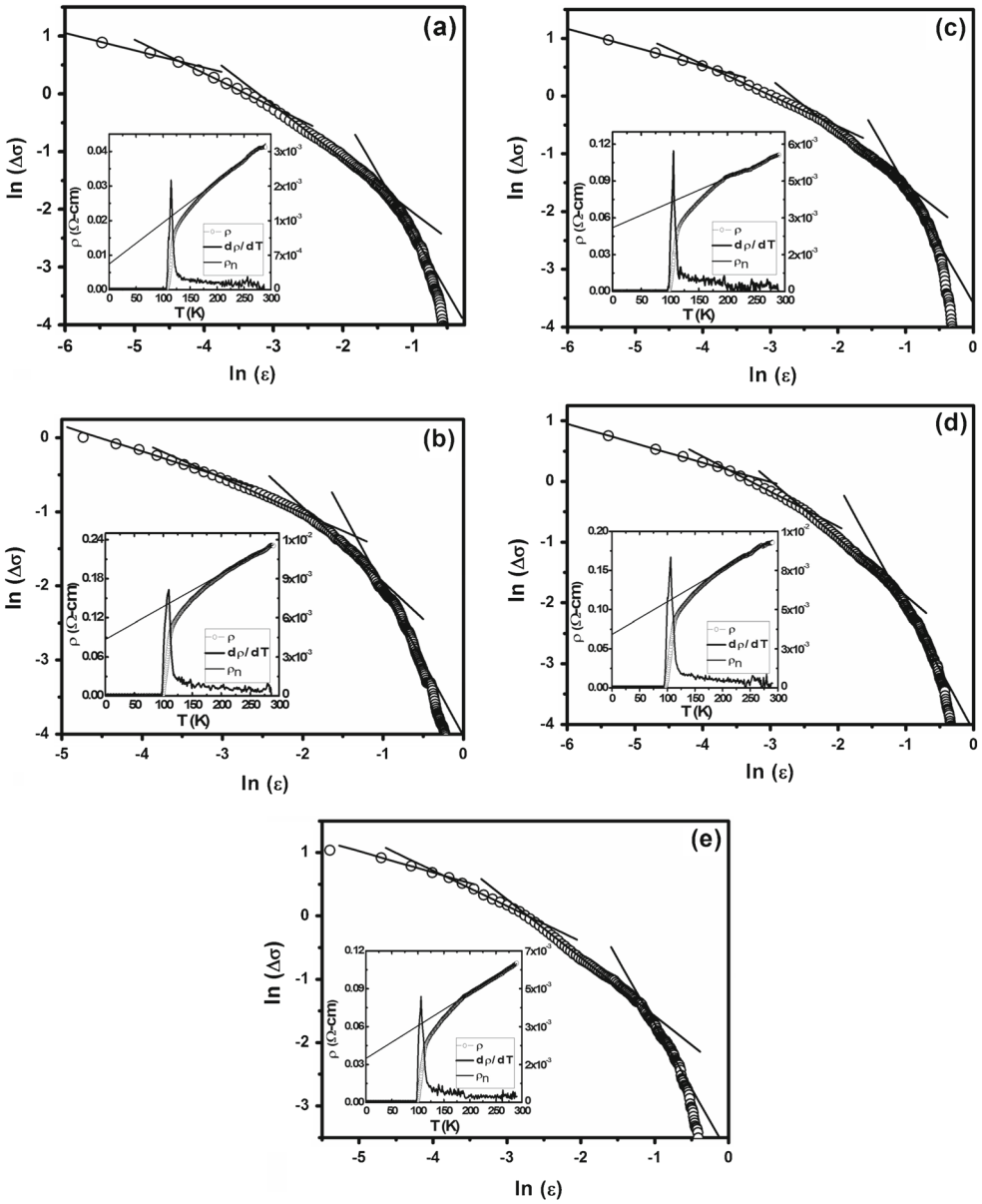

Fig. 6 **a**,**b**,**c**,**d**,**e** Log plot of the excess conductivity versus the reduced temperature

Table 1 Superconducting parameters estimated from excess conductivity

Sample	$\xi_{c(0)}$ (Å)	J	N_G	$\lambda_{p.d}$(Å)	$B_{c(0)}$ (T)	B_{c1} (T)	B_{c2} (T)	κ	$J_{c(0)}\times10^3$ (A/cm^2)	$V_F\times10^7$ (m/s)	E_{Break} (eV)	$\tau_\varphi\times10^{-14}$
Ti "0"	1.93	0.046	0.071	794.64	1.83	0.101	128.7	49.7	1.25	1.80	0.07	5.81
Ti "0.25"	3.58	0.158	0.142	2467.3	0.59	0.013	128.7	154.2	0.13	3.07	0.09	4.34
Ti "0.5"	2.84	0.100	0.118	1693.0	0.86	0.026	128.7	105.8	0.28	2.36	0.10	4.17
Ti "0.75"	2.50	0.077	0.153	1514.4	0.96	0.032	128.7	94.6	0.34	2.02	0.08	5.34
Ti "1.0"	2.35	0.068	0.095	1191.4	1.22	0.050	128.7	74.5	0.56	1.99	0.09	4.63

Table 2 Parameters estimated from $\ln(\Delta\sigma)$ and $\ln(\varepsilon)$ plots

Sample	λ_{CR}	λ_{3D}	λ_{2D}	λ_{SW}	T_{CR-3D} $=T_G$(K)	T3D-2D (K)	T2D-SW (K)	T_{cmf} (K)	T^*(K)	$\alpha = \rho_n$ (0 K) (Ω cm)	$W = \Delta T_c$ (K)
Ti "0"	0.30	0.55	0.97	2.06	116.2	120.1	146.8	114.8	164.7	0.007	6.28
Ti "0.25"	0.35	0.48	1.00	2.01	114.3	127.4	147.2	109.9	174.4	0.087	8.81
Ti "0.5"	0.32	0.53	0.99	2.03	108.5	117.2	145.3	106.5	166.6	0.051	7.26
Ti "0.75"	0.32	0.51	0.97	2.00	109.0	114.3	134.1	106.1	172.4	0.068	9.57
Ti "1.0"	0.33	0.54	0.98	2.04	108.5	113.8	143.8	106.5	164.2	0.034	8.38

conductivity regimes. By employing N_G and the Ginzburg-Landau theory, following important superconducting parameters are evaluated by using the equations of the following forms [15–17]:

$$N_G = \left|\frac{T_G - T_c^{mf}}{T_c^{mf}}\right| = 0.5\left[K_B T_c / B_{c(0)}^2 \gamma^2 \xi_{c(0)}^3\right]^2 \gamma \tag{3}$$

$$B_c = \frac{\Phi_0}{2\sqrt{2}\pi\lambda_{p.d(0)}\xi_{ab(0)}} \tag{4}$$

$$B_{c1} = \frac{B_c}{\kappa\sqrt{2}}\ln\kappa \tag{5}$$

$$B_{c2} = \sqrt{2}\kappa B_c \tag{6}$$

$$J_c = \frac{4\kappa B_{c1}}{3\sqrt{3}\lambda_{p.d(0)}\ln\kappa} \tag{7}$$

$$\tau_\varphi = \frac{\pi\hbar}{8k_B T\varepsilon_0} \tag{8}$$

The $\kappa = \lambda/\xi$, B_c, B_{c1}, B_{c2}, J_c, and τ_ϕ are the Ginzburg-Landau (GL) parameter, thermodynamic critical field, the lower critical field, the upper critical field, and the critical current density, respectively.

Using the phase relaxation time of the Cooper pairs τ_ϕ and the coupling constant $\lambda\lambda = \frac{\hbar\tau_\varphi^{-1}}{2\pi k_B T}$, the Fermi velocity of the carriers V_F and the energy E required to break up the Cooper pairs are determined by using equations of the following form:

$$V_F = \frac{5\pi k_B T_c \xi_{c(0)}}{2K\eta} \tag{9}$$

$$E = \frac{h}{\tau_\varphi(1.6\times10^{-19})} \tag{10}$$

The proportionality coefficient K used in the above equation (9) is 0.12 [18]. The values of parameters such as B_c, B_{c1}, $J_{c(0)}$, and τ_ϕ got decreased with increase in Ti doping. The parameters B_{c1} and $J_{c(0)}$ depend on B_c that in turn depend on the free energy difference between the normal and superconducting state. The suppression in the values of these parameters suggests that superconductivity volume fraction suppresses with the doping of Ti in the final compound. This also support our thesis that incorporation of Ti in the CuO_2 planes induces an-harmonic oscillation that suppresses the density of phonons and hence the superconductivity. These studies strongly suggest that role of electron-phonon interactions is essential in the mechanism of high-T_c superconductivity. Moreover, since the superconductivity is being influenced by the doping of Ti at the Cu sites, this shows that the role of soft phonon is essential for the high-T_c superconductivity.

4 Conclusions

$(Cu_{0.5}Tl_{0.5})Ba_2Ca_3(Cu_{4-x}Ti_x)O_{12-\delta}$ ($x = 0$, 0.25, 0.50, 0.75, 1.0) superconductors are prepared by two-step solid-state reaction method at 880 °C. The samples are characterized by X-ray diffraction, resistivity, AC susceptibility, and FTIR absorption measurements. These samples have shown tetragonal crystal structure with the a-axis length increasing, whereas the c-axis decreasing with increased Ti doping. The magnitude of superconductivity also suppresses with increase in Ti doping. FTIR absorption measurements of $(Cu_{0.5}Tl_{0.5})Ba_2Ca_3(Cu_{4-x}Ti_x)O_{12-\delta}$ ($x = 0$, 0.25, 0.50, 0.75, 1.0) samples have shown that the peak position of the apical oxygen modes at 480 and 540 cm^{-1} stays at the same position, whereas the CuO_2/TiO_2 planar oxygen modes is softened with increased Ti doping. The origin of softening of planar oxygen mode lies in decrease mass of doped the Ti (47.90 amu) atoms relative to the Cu (63.54 amu) atoms that results in increase of the bond length of the a-axis, and hence, these modes are softened. A possible correlation of suppression of superconductivity is attributed to the presence of atoms of different masses in CuO_2/TiO_2 planes which produce an-harmonic oscillations and hence suppress the density of phonon population. The phonons of harmonic oscillation with wave vector q and the an-harmonic oscillation with wave vector q' produces a new phonon with wave vector q that do not contribute in the Cooper pair formation. It suppresses the density of essential phonon

required for the Cooper pair formation and hence the superconductivity. These studies show the essential role of electron-phonon interactions in the mechanism of high-T_c superconductivity. Excess conductivity analyses (FIC) of these samples have shown that the transition width increases and the mean field critical temperature T_{cmf} is shifted to lower values with increased Ti doping. The increase in the coherence length along the c-axis, interlayer coupling, and the Fermi velocity of the carriers with Ti doping is reminiscence of decreased the c-axes length. The values of B_c, B_{c1}, $J_{c(0)}$, and τ_ϕ are, however, suppressed with increased Ti doping. Since the B_c determines the free energy difference between the normal and superconducting state, decreased values of it shows that superconducting volume fraction decreases with increased Ti doping. The excess conductivity analyses also support this thesis that density of phonon population suppresses with the Ti doping that result in suppression of the population of superconducting electrons, showing the essential role of electron-phonon interaction in the mechanism of high-T_c superconductivity. These studies have explicitly shown that soft phonon play an essential role in the high-T_c superconductivity.

References

1. Nawazish, A., Khan, A., Javaid, A.A., Khurran, N.H.: Phys. C **425**, 90 (2005)
2. Jergel, M., Conde Gallardo, A., Falcony Guajardo, C., Strbik, V.: upercond. Sci. Technol. **9**, 427 (1996)
3. Ibach, H., Lüth, H.: Solid-state physics: an introduction to theory and experiment. Springer (1993)
4. Christman, J.R.: Fundamentals of Solid Statem, 1st, p. 215. Wiley (1987)
5. Khan, N.A., Arif, M.: Physica C **488**, 35 (2013)
6. Mumtaz, M., Khan, N.A., Nawaz, R.: J. Supercond. Nov. Magn. **23**, 565–569 (2010)
7. Khan, N.A., Rahim, M.: J. Alloys Compd. **481**, 81 (2009)
8. Rahim, M., Khan, N.A.: J. Alloys Compd. **513**, 55 (2011)
9. Prade, J., Kulkarni, A.D., De Welte, F.W.: Phys. Rev. B **39**, 2771 (1989)
10. Kulkarni, A.D., De Welte, F.W., Prade, J., Schroder, U., Kress, W.: Phys. Rev. B **41**, 6409 (1990)
11. Sato, T., Nakane, H., Mori, N., Yoshizawa, S.: Phys. C **344**, 244 (2003)
12. Ghosh, A.K., Bandyopadhyay, S.K., Barat, P., Sen, P., Basu, A.N.: Phys. C **264**, 255 (1996)
13. Manmeet Kaur, R., Srinibasan, G.K., Mehta, D., Kanjilal, R., Pinto, S.B., Ogale, S., Mohan, V.G.: Phys. C **443**, 61 (2006)
14. Aslamazov, L.G., Larkin, A.L.: Phys. Lett. A **26**, 238 (1968)
15. Lawrence, W.E., Doniach, S.: In: Kanda, E. (ed.) Proceedings of the Twelfth International Conference on Low Temperature Physics, p. 361, Keigaku, Tokyo (1971)
16. Abu Aly, A.I., Ibrahim, I.H., Awad, R.A., El-Harizy, A.: J. Supercond. Nov. Magn. **23**, 1325 (2010)
17. Rojas Sarmiento, M.P., Uribe Laverde, M.A., Vera Lopez, E., Landinez Tellez, D.A., Roa-Rojas, J.: Phys. B **398**, 360 (2007)
18. Ben Azzouz, F., Zouaoui, M., Annabi, M., Ben Salem, M.: Sol. Stat. Phys. C **3**, 3048 (2006)
19. Solovjov, A.L., Dmitriev, V.M., Habermeier, H.-U.: Phys. Rev. B **55**, 8551 (1997)